Cardiovascular Research (2008) **79**, 448–457
doi:10.1093/cvr/cvn101

Epiblastic *Cited2* deficiency results in cardiac phenotypic heterogeneity and provides a mechanism for haploinsufficiency

Simon T. MacDonald[1†], Simon D. Bamforth[1†], Chiann-Mun Chen[1], Cassandra R. Farthing[1], Angela Franklyn[1], Carol Broadbent[1], Jürgen E. Schneider[1], Yumiko Saga[2], Mark Lewandoski[3], and Shoumo Bhattacharya[1]*

[1]*Department of Cardiovascular Medicine, University of Oxford, Wellcome Trust Centre for Human Genetics, Roosevelt Drive, Headington, Oxford OX3 7BN, UK;* [2]*Division of Mammalian Development, National Institute of Genetics, Yata 1111, Mishima 411-8540, Japan; and* [3]*Genetics of Vertebrate Development Section, National Cancer Institute, Frederick Cancer Research and Development Center, Box B, Building 539, Frederick, MD 21702, USA*

Received 29 October 2007; revised 27 March 2008; accepted 15 April 2008; online publish-ahead-of-print 25 April 2008

Time for primary review: 31 days

KEYWORDS
Cited2;
Cardiac development;
Phenotypic heterogeneity;
Haploinsufficiency;
Left–right patterning;
Pitx2c

Aims Deletion of the transcription factor *Cited2* causes penetrant and phenotypically heterogenous cardiovascular and laterality defects and adrenal agenesis. Heterozygous human *CITED2* mutation is associated with congenital heart disease, suggesting haploinsufficiency. *Cited2* functions partly via a *Nodal*→*Pitx2c* pathway controlling left–right patterning. In this present study we investigated the primary site of *Cited2* function and mechanisms of haploinsufficiency.
Methods and results A *Cited2* conditional allele enabled its deletion in particular cell lineages in mouse development. A *lacZ* reporter cassette allowed indication of deletion. Congenic *Cited2* heterozygous mice were used to investigate haploinsufficiency. Embryos were examined by magnetic resonance imaging, by sectioning and by quantitative real-time polymerase chain reaction (qRT-PCR). Epiblast-specific deletion of *Cited2* using *Sox2Cre* recapitulated penetrant and phenotypically heterogenous cardiovascular and laterality defects. Neural crest-specific deletion using *Wnt1Cre* affected cranial ganglia but not cardiac development. Mesodermal deletion with *Mesp1Cre* resulted in low penetrance of septal defect. Mesodermal deletion with *T-Cre* resulted in adrenal agenesis, but infrequent cardiac septal and laterality defects. β-Galatactosidase staining and qRT-PCR demonstrated the efficiency and location of *Cited2* deletion. Murine *Cited2* heterozygosity is itself associated with cardiac malformation, with three of 45 embryos showing ventricular septal defect. *Cited2* gene expression in E13.5 hearts was reduced 2.13-fold in $Cited2^{+/-}$ compared with wild-type ($P = 2.62 \times 10^{-6}$). The *Cited2* target gene *Pitx2c* was reduced 1.5-fold in $Cited2^{+/-}$ ($P = 0.038$) hearts compared with wild-type, and reduced 4.9-fold in $Cited2^{-/-}$ hearts ($P = 0.00031$). *Pitx2c* levels were reduced two-fold ($P = 0.009$) in $Cited2^{+/-}$ embryos, in comparison with wild-type. *Cited2* and *Pitx2c* expression were strongly correlated in wild-type and $Cited2^{+/-}$ hearts (Pearson rank correlation = 0.68, $P = 0.0009$). *Cited2* expression was reduced 7474-fold in *Sox2Cre* deleted hearts compared with controls ($P = 0.00017$) and *Pitx2c* was reduced 3.1-fold ($P = 0.013$). Deletion of *Cited2* with *Mesp1Cre* resulted in a 130-fold reduction in cardiac *Cited2* expression compared with control ($P = 0.0002$), but *Pitx2c* expression was not affected.
Conclusion These results indicate that phenotypically heterogenous and penetrant cardiac malformations in *Cited2* deficiency arise from a primary requirement in epiblast derivatives for left–right patterning, with a secondary cell-autonomous role in the mesoderm. Cardiac malformation associated with *Cited2* haploinsufficiency may occur by reducing expression of key *Cited2* targets such as *Pitx2c*.

*Corresponding author. Tel: +44 1865 287771; fax: +44 1865 287742.
E-mail address: shoumo.bhattacharya@well.ox.ac.uk
† These authors contributed equally to this work.

1. Introduction

The transcription factor *CITED2* binds the histone acetyltransferase CREBBP/EP300 with high affinity,[1] acting as a co-activator for transcription factors, such as TFAP2, LHX2, PPARA, and SMAD2/3.[2–5] It also acts as a repressor of hypoxia-activated transcription.[1] Genetic evidence indicates that *Cited2* is essential for cardiac, adrenal, neural, and placental development, and also for embryonic left–right patterning.[6–8] The cardiac malformations in mice lacking *Cited2* are highly penetrant and phenotypically heterogeneic, and include atrial, atrioventricular, and ventricular septal defects (ASD, AVSD, VSD), outflow tract defects [double outlet right ventricle (DORV), common arterial trunk (CAT), tetralogy of Fallot (TOF), transposition of great arteries (TGA)], and interrupted and right-sided aortic arch.[6,9] Mutation in *Cited2* also results in adrenal agenesis, fusion of cranial ganglia, abnormal cardiac neural crest migration, and exencephaly.[6]

In addition, *Cited2*$^{-/-}$ mice show left–right patterning defects characterized by right atrial and pulmonary isomerism, and abnormal ventricular topology at a lower penetrance.[7,8] Cardiovascular left–right patterning is created, in part, by the left-determining *Nodal*→*Pitx2c* pathway (reviewed by Hamada *et al.*[10] and Ramsdell[11]). Genetic evidence shows that *Cited2* is necessary for expression of *Pitx2c*, *Nodal*, and *Lefty2* in the left-lateral plate mesoderm and of *Lefty1* in the prospective floor plate, and is present at the promoter of the endogenous *Pitx2c* gene during development.[7,8] Thus, *Cited2* is necessary for *Nodal*-activated gene transcription.[7] The mechanism for the cardiovascular phenotypic heterogeneity and the partial penetrance of left–right patterning defect, which is observed even on a congenic *Cited2*-deficient background,[7] is not clear. Importantly, loss-of-function mutations in *CITED2* have been found in patients with phenotypically variable congenital heart disease.[12] These mutations are heterozygous, suggesting haploinsufficiency, but the mechanism for this is unclear.

Cited2 is expressed before gastrulation in the visceral endoderm.[13] Following gastrulation it is present in the newly forming mesoderm, developing blood islands, cardiac crescent, presomitic and splanchnic mesoderm, cranial neuroectoderm, and migrating neural crest before becoming ubiquitously expressed by embryonic day (E)8.5.[13] In the heart, it is highly expressed in the AV endocardial cushions.[8] One possible mechanism for cardiac phenotypic heterogeneity in *Cited2* deficiency is that not only is it required for the earlier process of left–right patterning but also independently for the later processes of atrioventricular septation, outflow tract, and aortic arch development.[8] Abnormal patterning of aortic arches and CAT observed in *Cited2* deficiency could, for instance, arise from defective neural crest development.[6] An alternative possibility is that an abnormality in the earlier developmental process of left–right patterning may secondarily affect the subsequent processes of atrioventricular septal, outflow tract, or aortic arch development.[7] These different mechanisms were investigated with a conditional knockout approach. We also investigated the mechanism of haploinsufficiency using quantitative analysis of *Cited2* and its target gene *Pitx2c*. We show that the phenotypic heterogeneity in *Cited2* deficiency is because of a primary requirement in epiblast derivatives with a secondary cell-autonomous role in the mesoderm. Also, *Cited2* haploinsufficiency may cause cardiac malformation by reducing expression of key *Cited2* targets such as *Pitx2c*.

2. Methods

2.1 Molecular biology

Standard molecular biology procedures were used for plasmid constructions.[14]

2.2 Generation of Cited2$^{flox/flox}$ mice

The targeting vector strategy and generation of correctly targeted embryonic stem cells with a conditional *Cited2* allele (*Cited2*^{flox} or *Cited2*^{f}) is shown in Supplementary material online, *Figure S1*. Methods are also provided in detail in the Supplementary data. The allele was designed such that, after successful *Cre* recombination, a *lacZ* expression cassette came under the control of the endogenous *Cited2* promoter. This allowed indication of efficient recombination by β-galactosidase staining.

2.3 Conditional deletion of *Cited2*

Cited2$^{+/-}$ mice (*Cited2*^{tm1Bha}) on a C57BL/6J background[7] were crossed with *Sox2Cre* (Tg(Sox2-cre)1Amc),[15] *Wnt1Cre* (Tg(Wnt1-cre)11Rth)[16] (both gifts from Andrew McMahon, Harvard University), *Mesp1Cre* (Mesp1tm2(cre)Ysa)[17] or *TCre*[18] mice to generate males with *Cited2*$^{+/-}$;*Cre* genotypes. These males were crossed to *Cited2*$^{flox/flox}$ females on a mixed 129Sv × C57BL/6J background to generate embryos with *Cited2*$^{-/flox}$;*Cre* and *Cited2*$^{+/flox}$;*Cre* (control) genotypes. This strategy prevented global recombination owing to *Cre* expression in the maternal germline.[19] *Cited2*$^{-/flox}$;*Cre* embryos lack *Cited2* expression in cells expressing *Cre*-recombinase. *Cited2*$^{+/flox}$;*Cre* embryos continue to express *Cited2*, providing littermate controls. Embryos were harvested at the indicated time points after the detection of a vaginal plug (E0.5), and genotyped using allele-specific polymerase chain reaction (PCR) (primer details are available on request). All mouse experiments conform with the *Guide for the Care and Use of Laboratory Animals* published by the National Institutes of Health (NIH Publication No. 85-23, revised 1996).

2.4 Analysis of embryos

Magnetic resonance imaging (MRI) was performed on a horizontal 9.4 T/21 cm VNMRS Direct Drive™ MR system (Varian Inc., Palo Alto, CA, USA) essentially as described previously[20] on embryos at E15.5. Whole mount *in situ* immunostaining was performed on E9.5 embryos using anti-neurofilament antibody (clone 2H3, Developmental Studies Hybridoma Bank, University of Iowa, IA, USA).[21] X-Gal and nuclear fast red (Sigma, St. Louis, MO, USA) staining were performed according to standard procedures.[14,16]

2.5 Quantitative real time-polymerase chain reaction

Embryo hearts (E13.5) were dissected out initially in DEPC treated phosphate-buffered saline (PBS), and then finely dissected in RNAlater (Ambion, Austin, TX, USA) to remove mediastinal tissue. Embryos at E8.5 were dissected free from the yolk sac in cold DEPC–PBS and flash-frozen in liquid nitrogen. RNA was isolated using a Nucleospin RNA purification kit (Clontech, Palo Alto, CA, USA), and an Archive cDNA kit (Ambion) used to synthesize complementary DNA. Quantitative RT-PCR (qRT-PCR) reactions were carried out using a Bio-Rad I-Cycler (Bio-Rad, CA, USA) and pre-optimized TaqMan® primer-probe sets from Applied Biosytems (*Mus musculus* assays Mm00516121_m1 (for NM_010828 *Cited2*),

Mm00440826_m1 (for NM_001042502 *Pitx2c*), and eukaryotic 18S rRNA). Expression levels were normalized to 18S rRNA using the R_0 method of analysis.[22,23] Multiplex reactions were performed with 18S rRNA and the TaqMan primer-probe set for the gene of interest. Data were normalized to the level obtained for 18S RNA in each case. All reactions were performed in triplicates and, as a quality control, only samples for which the threshold cycle (Ct) replicate values were within 1 Ct value of each other were used for subsequent analysis.[24] Mean values for each reaction triplicate were analysed.

2.6 Statistical analyses

We used the chi-squared test for deviation from expected Mendelian ratios (http://www.kursus.kvl.dk/shares/vetgen/_Popgen/genetik/applets/ki.htm), and calculated probability of a type I error using the CHIDIST function in Microsoft Excel (Redmond, WA, USA). For analysis of the qRT-PCR data, we used a two-tailed, two-sample heteroscedastic *t*-test assuming unequal variance.

3. Results

3.1 Deletion of *Cited2* in the epiblast

To determine the role of *Cited2* in the epiblast it was deleted using *Sox2Cre* which induces recombination in all epiblast cells by E6.5.[15]. Genotyping of mice at weaning showed a complete absence of *Cited2*$^{-/flox}$;*Sox2Cre* embryos, but genotyping at E15.5 showed that these embryos were present in the expected Mendelian ratio (Supplementary material online, *Table S1*). This indicated that *Cited2*$^{-/flox}$;*Sox2Cre* embryos die either in late gestation or perinatally. Two of 10 *Cited2*$^{-/flox}$;*Sox2Cre* embryos at E15.5 had visible exencephaly (not shown). Analysis of *Cited2*$^{-/flox}$;*Sox2Cre* embryos at E15.5 using MRI showed that they frequently had a classical cardiac laterality defect, i.e. right-atrial isomerism, associated with right-pulmonary isomerism (six of 10 embryos) (*Figure 1*; see also see Supplementary material online, *Table S2*), indicating a defect in embryonic left–right patterning. VSDs were present in all embryos (see Supplementary material online, *Table S2*). The embryos invariably had adrenal agenesis (see Supplementary material online, *Figure S2*). No defects were seen in the 11 littermate control *Cited2*$^{+/flox}$;*Sox2Cre* or in eight *Cited2*$^{-/flox}$ embryos.

3.2 Deletion of *Cited2* in the neural crest

To determine the requirement for *Cited2* in the neural crest it was deleted using *Wnt1Cre*, which drives expression of *Cre*-recombinase in all neural crest-derived tissues, including the cardiac neural crest, from E9.[16,25,26] There was a significant reduction in the numbers of *Cited2*$^{-/flox}$;*Wnt1Cre* mice in comparison with *Cited2*$^{+/flox}$;*Wnt1Cre* mice at weaning [21 of 61 vs. 40 of 61, respectively ($\chi^2 = 5.9$; $P < 0.015$). There was no observed reduction when genotyping was performed between E9.5 and E18.5. Examination of embryos at E15.5–E18.5 ($n = 16$) using MRI revealed none with heart or great vessel defects, but one embryo had exencephaly (*Figure 2B*). Exencephaly was not observed in *Cited2*$^{+/flox}$;*Wnt1Cre* embryos ($n = 16$). Examination of cranial ganglia by anti-neurofilament staining in *Cited2*$^{-/flox}$;*Wnt1Cre* embryos showed that 11 of 14 sets had fusions of ganglia IX and X (*Figure 2E* and *F*) and hypomorphic ganglia V and VII/VIII. In contrast, two of 28 sets of ganglia from *Cited2*$^{+/flox}$;*Wnt1Cre* embryos had fusions of ganglia IX and X ($\chi^2 = 22.28$; $P < 0.001$). In both *Cited2*$^{-/flox}$;*Wnt1Cre* and in *Cited2*$^{+/flox}$;*Wnt1Cre* embryos, we observed extensive *lacZ* staining in the cranial mesenchyme, and in the first and second pharyngeal arches

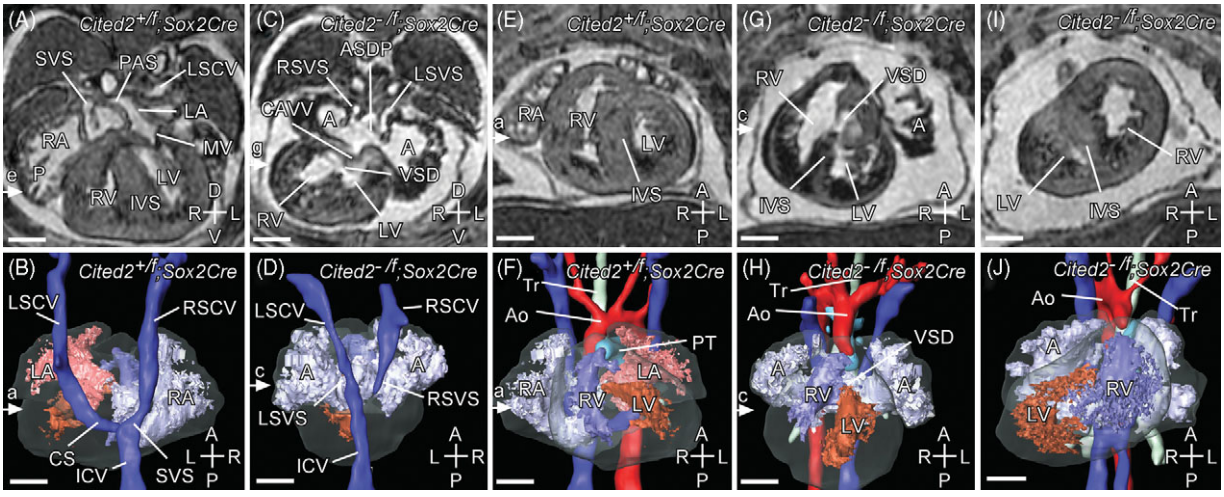

Figure 1 Deletion of *Cited2* in the epiblast: cardiac morphology. Magnetic resonance imaging of E15.5 embryos. (A–D) Transverse sections and three-dimensional (3D) reconstructions (dorsal views) of *Cited2*$^{+/flox}$;*Sox2Cre* (control) and *Cited2*$^{-/flox}$;*Sox2Cre* hearts. (*A*, *B*) Control normal heart showing a pectinated (P) right atrium (RA), with a systemic venous sinus (SVS), into which drains the right superior caval vein (RSCV), the left superior caval vein (LSCV) via the coronary sinus (CS) and the inferior caval vein (ICV). The left atrium (LA) is characterized by the primary atrial septum (PAS). Other structures seen are right and left ventricles (RV, LV), interventricular septum (IVS), and the mitral and tricuspid valves (MV, TV not labelled). (*C*, *D*) *Cited2*$^{-/flox}$;*Sox2Cre* heart showing a large primum atrial septal defect (ASDP), resulting in a common atrium (A). This is pectinated on each side and has bilateral systemic venous sinuses (LSVS, RSVS), into which drains the bilateral superior and inferior caval veins. The coronary sinus is absent. These appearances indicate right atrial isomerism. A common atrioventricular valve (CAVV) over-rides a ventricular septal defect (VSD). Note also that the heart is malpositioned to the right. (E–J) Coronal sections and 3D reconstructions (ventral views) of *Cited2*$^{+/flox}$;*Sox2Cre* (control) and *Cited2*$^{-/flox}$;*Sox2Cre* hearts. (*E*, *F*) Control normal heart where the right ventricle is dextral to the left, and gives rise to the main pulmonary trunk (PT). The left ventricle gives rise to the aorta (Ao), which arches to the left of the trachea (Tr) over the left main bronchus. (*G*, *H*) *Cited2*$^{-/flox}$;*Sox2Cre* heart with normal ventricular topology, cardiac dextroposition, and a right-sided aortic arch arising from the right ventricle. (*I*, *J*) *Cited2*$^{-/flox}$;*Sox2Cre* heart with abnormal ventricular topology: the right ventricle is sinistral (and anterior) to the left ventricle. Scale bars = 500 μm; axes: D, dorsal; V, ventral; R, right; L, left; A, anterior; P, posterior.

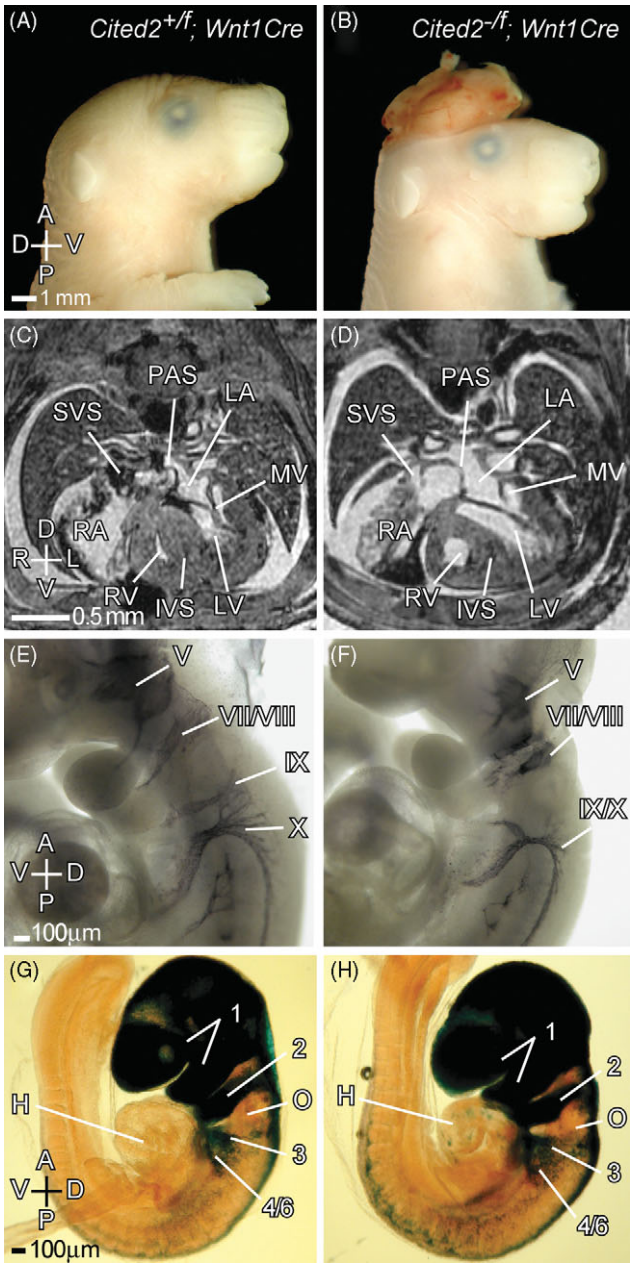

Figure 2 Deletion of *Cited2* in the neural crest. Control (*Cited2*$^{+/flox}$*;Wnt1Cre*, left panels) and mutant (*Cited2*$^{-/flox}$*;Wnt1Cre*, right panels) embryos were analysed at different stages of development. (*A*, *B*) Control and mutant E17.5 embryos, respectively. The mutant embryo has exencephaly. (*C*, *D*) Magnetic resonance imaging (MRI) transverse sections of E17.5 control and mutant embryos. No cardiac or aortic arch abnormalities were identified in 14 mutant embryos examined by MRI. (*E*, *F*) Anti-neurofilament antibody staining of control and mutant E9.5 embryos showing cranial ganglia. The fifth (trigeminal ganglion) is smaller, and the ninth and tenth (glossopharyngeal and vagal) ganglia are fused in the mutant. (*G*, *H*) *LacZ* staining of control and mutant embryos. Extensive staining is observed in the cranial mesenchyme, and in the first and second pharyngeal arches. Staining is also observed in the cardiac neural crest (the third and fourth/sixth pharyngeal arches). No difference was observed in either case. The otic vesicle (O) is indicated. Axes and abbreviations are as shown in *Figure 1*.

(*Figure 2G* and *H*). Staining was also observed in the cardiac neural crest (the third and fourth/sixth pharyngeal arches). The staining pattern corresponded to that described with *Wnt1Cre*-driven recombination in R26R mice that express *lacZ* conditional to *Cre*-mediated recombination.[16]

3.3 Deletion of *Cited2* in the mesoderm

The role of *Cited2* in the cranial, cardiac, and extraembryonic mesoderm was examined by deletion using crosses with *Mesp1Cre* mice, which deletes in these tissues by E7.5.[17,27] As this *Cre* allele is a 'knockin' and disrupts the endogenous gene, we analysed genotypic ratios of offspring born by crossing these lines with *Cited2*$^{+/-}$ mice to determine if there was a genetic interaction. The number of *Cited2*$^{+/-}$*; Mesp1Cre*$^{+/KI}$ mice at weaning was similar to *Cited2*$^{+/+}$*; Mesp1Cre*$^{+/KI}$ mice indicating no significant genetic interaction (Supplementary material online, *Table S3*). Isolated septal defects (but no outflow or aortic arch defects) were seen in three of 18 *Cited2*$^{-/flox}$*;Mesp1Cre* embryos and no defects were seen in the seven *Cited2*$^{+/flox}$*;Mesp1Cre* or nine *Cited2*$^{-/flox}$ littermate control embryos studied (Supplementary material online, *Figure S3*). The deletion of *Cited2* using a *TCre* driver was then investigated. This would be expected to delete extensively in the lateral-plate, intermediate, and paraxial mesoderm and the hindgut endoderm, with earliest deletion being detected by E7.5[18]. Deletion of *Cited2* using *TCre* resulted in frequent adrenal agenesis (10 of 14 embryos), and infrequent cardiac septal and left–right patterning defect (three of 14 and one of 14, respectively, *Figure 3*). No defects were identified in the 11 *Cited2*$^{+/flox}$*;TCre* littermate control embryos studied.

3.4 Analysis of *Cited2* recombination

3.4.1 *LacZ* staining

The above results indicate that *Cited2* deficiency induced by *Wnt1Cre*, *Mesp1Cre*, or *TCre* drivers cannot explain either the phenotypic heterogeneity or penetrance of cardiac malformation and left–right patterning defects observed in the epiblast-specific deletion of *Cited2*. To explore the mechanism and evaluate the efficiency of recombination we examined the expression of *lacZ* in these different *Cited2*$^{+/flox}$*;Cre* embryos at E9.5 in comparison with *Cited2*$^{+/flox}$*;Sox2Cre* (*Figure 4* and Supplementary material online, *Table S4*). Deletion of exon 2 by *Cre*-recombinase brings the *lacZ* cassette under control of the endogenous *Cited2* promoter, so analysis of *lacZ* expression allowed the confirmation of *Cited2*^{flox} recombination in the embryonic lineages where both the *Cre* driver and *Cited2* are expressed. In the heart, we observed staining resembling the *Sox2Cre* pattern using *Mesp1Cre*, consistent with effective recombination in the cardiogenic mesoderm.[17,27] Reduced *lacZ* staining was observed in the outer curvature of the left ventricle suggesting that *Cited2* is not highly expressed here (*Figure 4*). With *TCre* we observed complete recombination in the common atrial chamber, but partial recombination in the atrioventricular canal, primitive ventricle, bulbus cordis, and outflow tract. The lateral plate mesoderm is thought to play a key role in establishing left–right patterning (reviewed in Hamada *et al.*[10]). We therefore examined the expression of *lacZ* in structures derived from the lateral plate mesoderm: these include the mesenchyme of the body wall (somatopleure) and of the viscera (splanchnopleure).[28] In *Cited2*$^{+/flox}$*;Sox2Cre* embryos, strong *lacZ* expression was observed in the splanchnopleure, and weaker expression in the somatopleure. With *TCre* and *Mesp1Cre*, *lacZ* expression was detected chiefly in the posterior splanchnopleure surrounding the midgut. No *lacZ* staining was detected in the somatopleure.

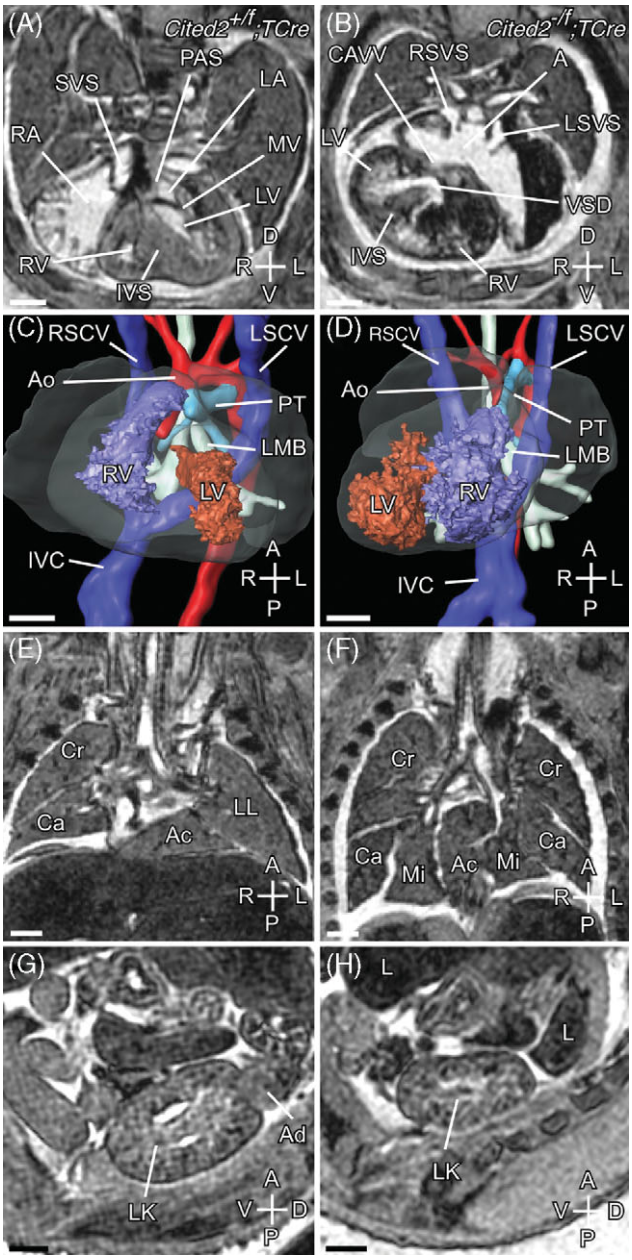

Figure 3 Deletion of *Cited2* using *TCre*. Control (*Cited2*$^{+/flox}$*;TCre*, left panels) and mutant (*Cited2*$^{-/flox}$*;TCre*, right panels) embryos were analysed at E15.5 using magnetic resonance imaging. (*A*) Transverse section of a control embryo showing normal cardiac anatomy. (*B*) Corresponding transverse section from the single mutant embryo (of 14 analysed) that showed a laterality defect. Right atrial isomerism is indicated by bilateral systemic venous sinuses and a common atrium created by complete absence of the primary atrial septum. The heart is dextroposed, with abnormal ventricular topology [dextral left ventricle (LV)] and a ventricular septal defect. (*C*) Three-dimensional (3D) reconstruction of the control embryo heart showing normal topology of the ventricles. The aorta (Ao) arises from the LV, and pulmonary trunk (PT) from the right ventricle (RV). Both Ao and PT arch over the left main bronchus (LMB). (*D*) 3D reconstruction of the mutant embryo heart showing abnormal ventricular topology. Both Ao and PT arise from the RV and arch over the LMB. (*E*) Sagittal section through the control embryo showing normal pulmonary topology. The three lobes of the right lung are seen. The left lung (LL) has a single lobe. (*F*) Sagittal section through the mutant embryo showing right pulmonary isomerism. Both lungs have three lobes. A fused accessory (Ac) lobe is also seen. (*G*, *H*) Sagittal sections through the left kidney (LK) of control and mutant embryos, respectively. The adrenal gland (Ad) is seen in the control but not in the mutant embryo. Scale bars = 500 μm. Axes and abbreviations are as shown in *Figure 1*.

We also examined *lacZ* expression at earlier developmental stages (Supplementary material online, *Figure S4*). At earlier stages, in *Cited2*$^{+/flox}$*;Sox2Cre* embryos at E7.5, *lacZ* expression was present in all epiblast-derived tissues, including the extraembryonic mesoderm. In *Cited2*$^{+/flox}$*;TCre* embryos, we observed *lacZ* staining in the extraembryonic mesoderm, amnion, and blood islands, and also to some extent in the nascent embryonic mesoderm. This became more extensive in the primitive streak and migrating embryonic mesoderm at slightly later stages. Examination of head-fold stage *Cited2*$^{+/flox}$*;Mesp1Cre* embryos showed extensive recombination in the cardiac crescent (Supplementary material online, *Figure S4*).

3.4.2 Quantitative real-time polymerase chain reaction

To verify efficient deletion of *Cited2* in the *Sox2Cre* and *Mesp1Cre* conditional knockouts at the mRNA level, and to determine the effect on the *Cited2* target gene *Pitx2c*, qRT-PCR was performed. *Cited2* expression was reduced 7474-fold ($P = 0.00017$) in *Cited2*$^{-/flox}$*;Sox2Cre* hearts compared with littermate controls (*Figure 5A*). There was also a 3.1-fold reduction in *Pitx2c* expression ($P = 0.013$; *Figure 5B*). *Cited2* expression was reduced 130-fold in *Cited2*$^{-/flox}$*;Mesp1Cre* hearts compared with littermate controls (*Figure 5C*). However, no reduction in *Pitx2c* expression was seen in these hearts (*Figure 5D*).

3.5 *Cited2* haploinsufficiency in the mouse

The mutations found in human congenital heart disease patients[12] suggested that *Cited2* haploinsufficiency may occur. We tested for this in the mouse by examining the genotypic ratios of *Cited2*$^{+/-}$ intercrosses where we obtained 500 wild-type and 782 *Cited2*$^{+/-}$ pups (expected 855). The 8.5% reduction in *Cited2*$^{+/-}$ pups was statistically significant ($\chi^2 = 18.5$; $P < 0.0001$). A similar reduction was not observed however when the genotypic ratios of E13.5 or E15.5 embryos were examined (Supplementary material online, *Table S5*).

To determine a mechanism for reduced survival, we examined *Cited2*$^{+/-}$ embryos at E15.5 by MRI (*Figure 6*). This was followed by histological sectioning of embryos that had either oedema or a cardiac abnormality visible on MRI. We found that three of 45 *Cited2*$^{+/-}$ embryos had a clearly identifiable VSD, and one presented with DORV with hypoplastic pulmonary trunk (*Figure 6*). These defects were not seen in the wild-type littermate controls. Thus, heterozygosity for a *Cited2* null allele is associated, at low penetrance, with cardiac malformation in the mouse, implying haploinsufficiency.

3.6 Quantitative real-time-polymerase chain reaction analysis of *Pitx2c* and *Cited2* expression

To determine if haploinsufficiency in *Cited2*-deficient hearts is linked to abnormality in *Pitx2c* expression, we examined gene expression using qRT-PCR. Embryos and hearts on a C57BL/6J background, generated by backcrossing for 14 generations, were used to minimize the effects of genetic background. Hearts at E13.5 were used as this is a key timepoint in cardiac septation, and embryos at E8.5 were selected as *Pitx2c* is expressed asymmetrically in the left lateral plate mesoderm at this stage. In E13.5 hearts, *Cited2* was reduced 2.13-fold in *Cited2*$^{+/-}$ compared with

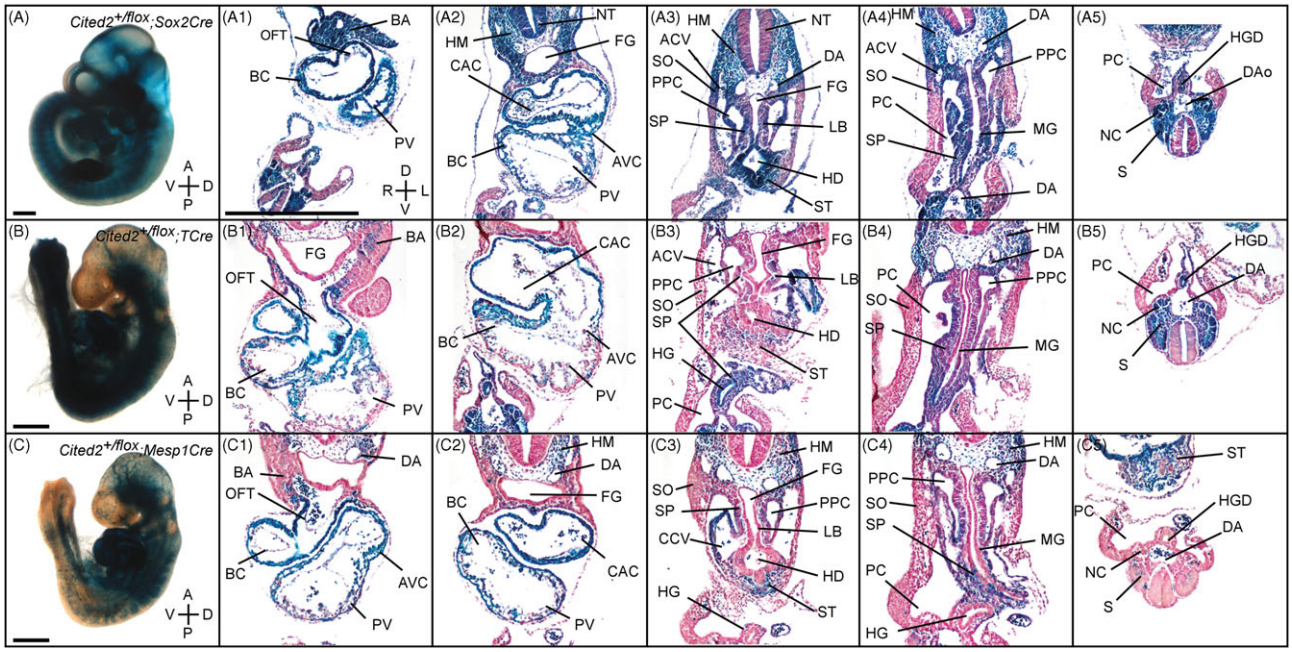

Figure 4 *LacZ* expression in *Cited2*$^{+/flox}$*;Cre* embryos. The left panels show pictures of embryos (E9.5) with the indicated genotypes after staining for *lacZ*. Subsequent panels show transverse embryo sections counterstained with nuclear fast red. ACV, anterior cardinal vein; AVC, atrioventricular canal; BA, branchial arch; BC, bulbus cordis; CAC, common atrial chamber; CCV, common cardinal vein; DA, dorsal aorta; FG, foregut; HD, hepatic diverticulum; HG, hindgut; HGD, hindgut diverticulum; HM, head mesenchyme; LB, lung bud; LM, lateral mesenchyme from splanchnopleure; MG, midgut; NC, nephric cord (intermediate mesenchyme); NT, neural tube; OFT, outflow tract; PC, peritoneal cavity; PPC, pleuroperitoneal canal; PV, primitive ventricle; ST, septum transversum; S, somite. Scale bars = 500 μm. Axes are as shown in *Figure 1*.

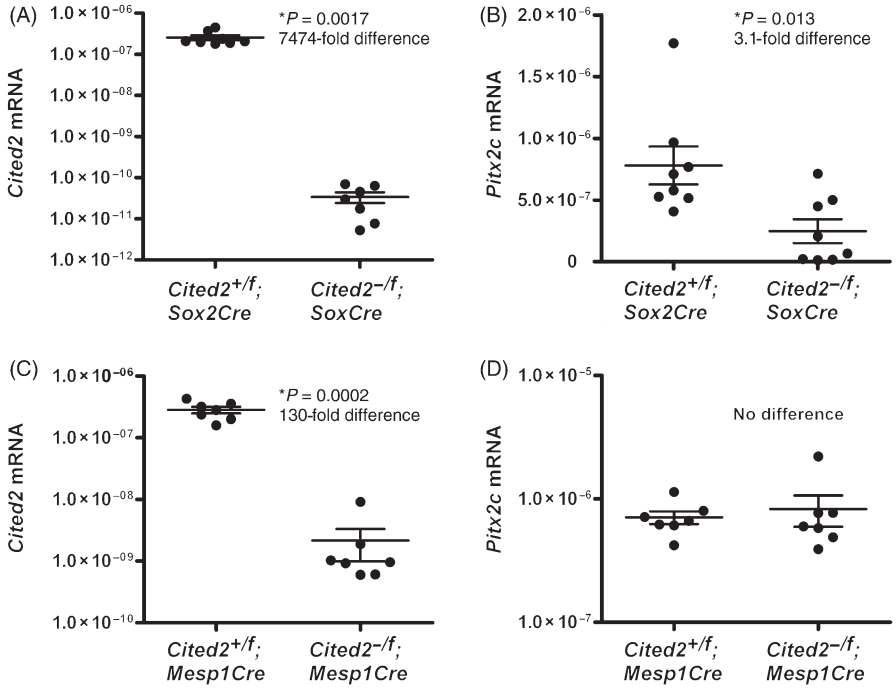

Figure 5 *Cited2* and *Pitx2c* mRNA levels in *Cited2* conditionally deleted hearts at E13.5. Sample mean and SEM are indicated. (*A*) *Cited2* mRNA levels were reduced 7474-fold in *Cited2*$^{-/flox}$*;Sox2Cre* hearts compared with controls. (*B*) A significant 3.1-fold decrease in *Pitx2c* mRNA levels was found in *Cited2*$^{-/flox}$*;Sox2Cre* hearts compared with controls. (*C*) In *Cited2*$^{-/flox}$*;Mesp1Cre* hearts, *Cited2* levels were reduced 130-fold compared with controls. (*D*) No significant difference in *Pitx2c* expression was found between *Cited2*$^{-/flox}$*;Mesp1Cre* hearts and controls.

wild-type ($P = 2.62 \times 10^{-6}$) (*Figure 7A*). We found that the *Cited2* mRNA in *Cited2*$^{-/-}$ hearts was either undetectable or, if detectable, had values ranging between 1.45×10^{-12} and 3.47×10^{-11} relative to 18S (*Figure 7C*), likely to represent the limits of the assay. The *Cited2* target gene *Pitx2c* was reduced 1.5-fold in *Cited2*$^{+/-}$ ($P = 0.038$) hearts and 4.7-fold ($P = 0.00031$) in *Cited2*$^{-/-}$ hearts compared with wild-type controls (*Figure 7B* and *D*). *Cited2* and *Pitx2c* mRNA were strongly correlated in wild-type and *Cited2*$^{+/-}$ hearts (Pearson rank correlation = 0.68, $P =$

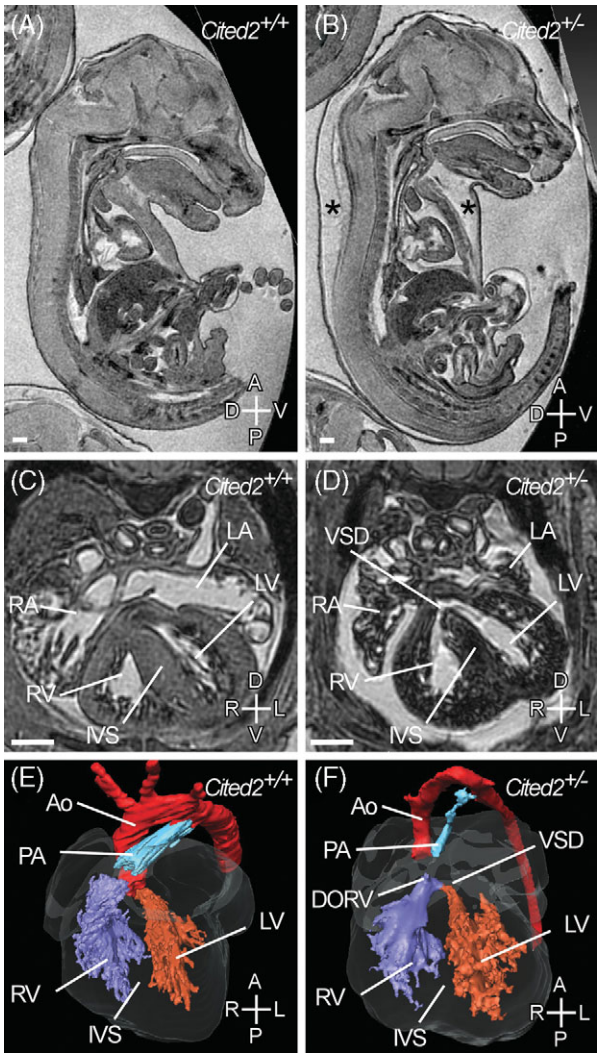

Figure 6 Oedema and cardiac malformations in *Cited2*$^{+/-}$ embryos. Magnetic resonance imaging of wild-type and littermate *Cited2*$^{+/-}$ embryos at E15.5. Sagittal sections of wild-type (*A*) and *Cited2*$^{+/-}$ (*B*) embryos. Severe oedema (asterisks) is seen in the *Cited2*$^{+/-}$ embryo. (*C*) Transverse section of wild-type and *Cited2*$^{+/-}$ embryos. The *Cited2*$^{+/-}$ embryo has a ventricular septal defect (VSD) (*D*). (*E, F*) Three-dimensional reconstruction of the heart in the wild-type and *Cited2*$^{+/-}$ embryos shown in the previous panel. The aorta (Ao) and pulmonary artery (PA) arise from the left ventricle and right ventricle (RV), respectively, in the wild-type embryo, but in the *Cited2*$^{+/-}$ embryo they arise from the RV creating a double-outlet right ventricle (DORV). VSD is indicated. Scale bars, 500 μm. Axes are as shown in *Figure 1*.

0.0009; *Figure 7F*). In the E8.5 embryos, we found a two-fold reduction in *Pitx2c* levels in *Cited2*$^{+/-}$ compared with wild-type ($P = 0.009$; *Figure 7E*).

4. Discussion

In these experiments, we used a conditional knockout approach to understand how *Cited2* deficiency results in cardiac phenotypic heterogeneity. To define the role of *Cited2* in the epiblast, we deleted it with *Sox2Cre*.[15] This resulted in 100% penetrance of cardiovascular malformations and adrenal agenesis. The most common cardiac malformation was a VSD, which was present in all embryos, and was associated with DORV in some embryos. In addition we observed left–right patterning, atrial septal, outflow tract, and aortic arch defects. These observations are consistent with, and fully recapitulate, those previously reported with the global deletion of *Cited2*.[6–9,29] They indicate that *Cited2* is essential in the epiblast or its derivatives for normal embryonic left–right patterning, and for cardiac and adrenal development. The complete penetrance of the defects, and the widespread expression of *lacZ* in embryos containing a *Cited2*^{flox} allele and the *Cre* transgene also indicate that efficient recombination occurs in response to *Cre* expression. This was further validated by the large reduction seen in *Cited2* mRNA levels in the hearts of *Cited2*$^{-/flox}$*;Sox2Cre* embryos. We observed reduced *lacZ* staining in the outer curvature of the left ventricle following conditional deletion of *Cited2* with *Sox2Cre* (as well as with *Mesp1Cre* and *TCre*). This is consistent with the published data,[8] and indicates that *Cited2* is expressed at a lower level in this region of the heart.

To define the role of *Cited2* in the neural crest, we deleted it with *Wnt1Cre*.[16,30] This resulted in cranial ganglia fusions and exencephaly, but did not affect cardiac septal, outflow tract, aortic arch or adrenal development, or left–right patterning. These results indicate that although *Cited2* does have a cell autonomous role in the neural crest, as evidenced by fusion of the cranial ganglia, it is not required here for outflow tract septation or aortic arch patterning.

To determine the requirement of *Cited2* in the cranial, cardiac, and extraembryonic mesoderm it was deleted with *Mesp1Cre*, which results in extensive recombination in these tissues by E7.5.[17,27] Subsequently, by E9.5, recombination is observed extensively in myocardium and endocardium including the mesenchyme of the cono-truncal and atrioventricular cushions, in the epicardium, and in the pharyngeal arch mesoderm and vascular endothelium.[17,27,31] Deletion of *Cited2* using *Mesp1Cre* resulted in low penetrance of septal defect, and no outflow tract, aortic arch, or laterality defects. These results indicate that *Cited2* function in the mesoderm does not explain the phenotypically heterogeneic cardiac malformations observed in the epiblast-specific deletion. Efficient recombination at the *Cited2* locus in response to *Cre* expression as demonstrated by *lacZ* staining and qRT-PCR indicated that lack of a phenotypically heterogeneic phenotype is unlikely to be owing to inefficient recombination.

As *Cited2* is expressed in the lateral-plate mesoderm,[8] and as its deficiency also leads to loss of *Nodal*-activated transcripts such as a *Nodal*, *Lefty2*, and *Pitx2c* in the left-lateral plate mesoderm,[7,8] we investigated its role here by deletion using *TCre*.[18] This resulted in infrequent septal and laterality defect. Deletion of *Cited2* induced by *TCre* was predominantly in the posterior rather than the anterior extent of the lateral plate mesoderm, making this one possible mechanism for the infrequency of left–right patterning defect observed with a *TCre*-induced deletion. The *lacZ* staining pattern seen in *Cited2*$^{+/flox}$*;TCre* embryos was comparable with that seen with *TCre* × *R26R lacZ* embryos.[18] Moreover, in the heart the staining pattern was highly reminiscent of that observed for *Isl1*[32] suggesting that *TCre* may also drive recombination in second heart field-derived regions of the heart. These results indicate that the penetrant and phenotypically heterogeneic cardiac malformations in *Cited2* deficiency arise from a primary requirement in epiblast derivatives for left–right

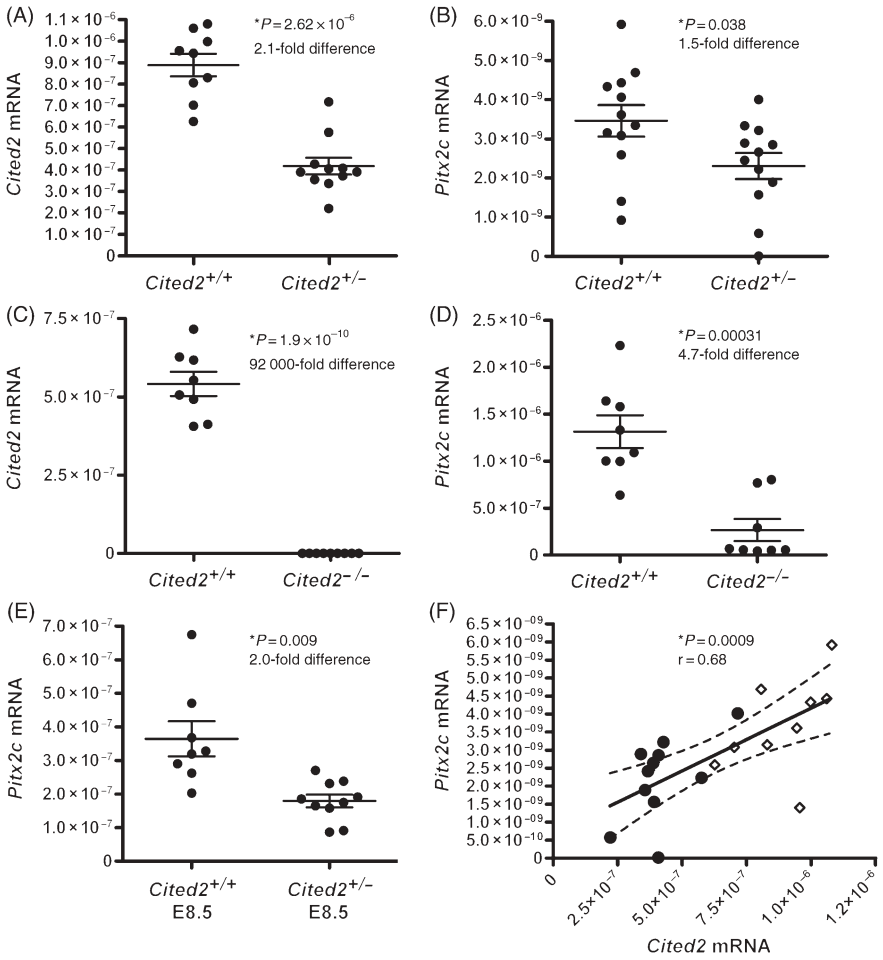

Figure 7 *Cited2* and *Pitx2c* mRNA levels in E13.5 embryo hearts and E8.5 embryos. Sample mean and SEM are indicated. (*A*) A 2.1-fold reduction in *Cited2* mRNA levels was seen in *Cited2*$^{+/-}$ hearts compared with wild-type. (*B*) *Pitx2c* levels were reduced 1.5-fold in *Cited2*$^{+/-}$ hearts compared with wild-type. (*C*) A 92 000-fold reduction in *Cited2* mRNA is seen in the *Cited2*$^{-/-}$ hearts compared with wild-type. (*D*) *Pitx2c* mRNA levels were reduced 4.7-fold in the *Cited2*$^{-/-}$ hearts compared with wild-type. (*E*) *Pitx2c* levels in wild-type and *Cited2*$^{+/-}$ E8.5 embryos. A two-fold reduction in *Pitx2c* mRNA is seen in the *Cited2*$^{+/-}$ embryos. (*F*) Pearson correlation between *Cited2* and *Pitx2c* E13.5 heart mRNA levels with line-of-best-fit and 95% confidence intervals (dotted lines) shown. Filled circles represent data from *Cited2*$^{+/-}$ hearts and diamonds those from wild-type. *Cited2* and *Pitx2c* mRNA levels were strongly correlated in wild-type and *Cited2*$^{+/-}$ hearts.

patterning with a secondary cell-autonomous role in the mesoderm for septation. A limitation of our studies, however, is that the role of *Cited2* in the endoderm—which has a major role in cardiac induction[33]—could not be established. We are currently limited here by the lack of a suitable *Cre* driver that expresses in the endoderm at the appropriate time-point.

Our data also show that *Cited2* haploinsufficiency occurs in the mouse and is associated with cardiac malformation. Although 8.5% of *Cited2* heterozygous pups are lost by weaning, consistent with the numbers of cardiac malformations observed, no deviation from expected numbers was seen during development. The mechanistic link between cardiac malformations and *Cited2* haploinsufficiency is unclear, and to address this, we quantitatively examined the expression of *Cited2* and its target gene *Pitx2c* in embryonic hearts and E8.5 embryos. Using qRT-PCR we showed that *Cited2* expression is significantly reduced in *Cited2* heterozygous embryonic hearts. We also showed that this was accompanied by a significant reduction in *Pitx2c* expression, and that the two were strongly correlated. We also observed a significant reduction in *Pitx2c* levels in E8.5 *Cited2*$^{+/-}$ embryos. As the dose of *Pitx2c* is crucial for normal left–right patterning and cardiac development,[34,35] we suggest that *Pitx2c* deficiency observed in *Cited2* heterozygous hearts and embryos could explain, at least in part, the observed cardiac malformations.

In conclusion, these results indicate that phenotypically heterogeneic and penetrant cardiac malformations in *Cited2* deficiency arise from a primary requirement in epiblast derivatives for left–right patterning with a secondary cell-autonomous role in the mesoderm for septation. Cardiac malformation associated with *Cited2* haploinsufficiency may occur by reducing the expression of key *Cited2* targets, such as *Pitx2c* from E8.5. Importantly, cardiovascular phenotypic heterogeneity is observed, for instance, with mutation in *NKX2-5*,[36–38] *CFC1*[39,40] or *ZIC3*.[41–43] Consistent with our proposed model, these genes, like *Cited2*, are also known to control or modulate left–right patterning pathways.[42,44–47] Our results support the emerging idea[7,11] that genes controlling early left–right patterning are candidates for diverse forms of human congenital heart disease, even in the absence of a classical laterality defect such as isomerism.

Supplementary material

Supplementary material is available at *Cardiovascular Research* online.

Acknowledgements

We thank Stuart Peirson for advice on quantitative real-time polymerase chain reaction and Hannah Barnes for technical help with magnetic resonance imaging.

Conflict of interest: none declared.

Funding

The Wellcome Trust (Grant 054528), the British Heart Foundation (Grant PG/06/075/21127), and the Center for Cancer Research, National Cancer Institute. S.T.M. is a Wellcome Trust Prize Student (Grant 076257/Z/04/Z) and S.B. a Wellcome Trust Senior Research Fellow.

References

1. Bhattacharya S, Michels CL, Leung MK, Arany ZP, Kung AL, Livingston DM. Functional role of p35srj, a novel p300/CBP binding protein, during transactivation by HIF-1. *Genes Dev* 1999;**13**:64–75.
2. Braganca J, Eloranta JJ, Bamforth SD, Ibbitt JC, Hurst HC, Bhattacharya S. Physical and functional interactions among AP-2 transcription factors, p300/CREB-binding protein, and CITED2. *J Biol Chem* 2003;**278**:16021–16029.
3. Glenn DJ, Maurer RA. MRG1 binds to the LIM domain of Lhx2 and may function as a coactivator to stimulate glycoprotein hormone alpha-subunit gene expression. *J Biol Chem* 1999;**274**:36159–36167.
4. Tien ES, Davis JW, Vanden Heuvel JP. Identification of the CREB-binding protein/p300-interacting protein CITED2 as a peroxisome proliferator-activated receptor alpha coregulator. *J Biol Chem* 2004;**279**: 24053–24063.
5. Chou YT, Wang H, Chen Y, Danielpour D, Yang YC. Cited2 modulates TGF-beta-mediated upregulation of MMP9. *Oncogene* 2006;**25**:5547–5560.
6. Bamforth SD, Braganca J, Eloranta JJ, Murdoch JN, Marques FI, Kranc KR *et al*. Cardiac malformations, adrenal agenesis, neural crest defects exencephaly in mice lacking Cited2 a new Tfap2 co-activator. *Nat Genet* 2001;**29**:469–474.
7. Bamforth SD, Braganca J, Farthing CR, Schneider JE, Broadbent C, Michell AC *et al*. Cited2 controls left-right patterning and heart development through a Nodal→Pitx2c pathway. *Nat Genet* 2004;**36**:1189–1196.
8. Weninger WJ, Floro KL, Bennett MB, Withington SL, Preis JI, Barbera JP *et al*. Cited2 is required both for heart morphogenesis and establishment of the left-right axis in mouse development. *Development* 2005;**132**: 1337–1348.
9. Yin Z, Haynie J, Yang X, Han B, Kiatchoosakun S, Restivo J *et al*. The essential role of Cited2, a negative regulator for HIF-1{alpha}, in heart development and neurulation. *Proc Natl Acad Sci USA* 2002;**99**: 10488–10493.
10. Hamada H, Meno C, Watanabe D, Saijoh Y. Establishment of vertebrate left-right asymmetry. *Nat Rev Genet* 2002;**3**:103–113.
11. Ramsdell AF. Left-right asymmetry and congenital cardiac defects: getting to the heart of the matter in vertebrate left-right axis determination. *Dev Biol* 2005;**288**:1–20.
12. Sperling S, Grimm CH, Dunkel I, Mebus S, Sperling HP, Ebner A *et al*. Identification and functional analysis of CITED2 mutations in patients with congenital heart defects. *Hum Mutat* 2005;**26**:575–582.
13. Dunwoodie SL, Rodriguez TA, Beddington RSP. Msg1 and Mrg1, founding members of a gene family, show distinct patterns of gene expression during mouse embryogenesis. *Mech Dev* 1998;**72**:27–40.
14. Ausubel F, Brent R, Kingston RE, Moore DD, Seidman JG, Smith JA *et al*. *Short Protocols in Molecular Biology*. Hoboken: John Wiley & Sons, Inc.; 1995.
15. Hayashi S, Lewis P, Pevny L, McMahon AP. Efficient gene modulation in mouse epiblast using a Sox2Cre transgenic mouse strain. *Mech Dev* 2002;**119**(Suppl. 1):S97–S101.
16. Jiang X, Rowitch DH, Soriano P, McMahon AP, Sucov HM. Fate of the mammalian cardiac neural crest. *Development* 2000;**127**:1607–1616.
17. Saga Y, Miyagawa-Tomita S, Takagi A, Kitajima S, Miyazaki J, Inoue T. MesP1 is expressed in the heart precursor cells and required for the formation of a single heart tube. *Development* 1999;**126**:3437–3447.
18. Perantoni AO, Timofeeva O, Naillat F, Richman C, Pajni-Underwood S, Wilson C *et al*. Inactivation of FGF8 in early mesoderm reveals an essential role in kidney development. *Development* 2005;**132**:3859–3871.
19. Hayashi S, Tenzen T, McMahon AP. Maternal inheritance of Cre activity in a Sox2Cre deleter strain. *Genesis* 2003;**37**:51–53.
20. Schneider JE, Bose J, Bamforth SD, Gruber AD, Broadbent C, Clarke K *et al*. Identification of cardiac malformations in mice lacking Ptdsr using a novel high-throughput magnetic resonance imaging technique. *BMC Dev Biol* 2004;**4**:16–27.
21. Wilkinson DG. Whole mount in situ hybridization of vertebrate embryos. In: Wilkinson DG (ed.), *In situ Hybridization*. Oxford: IRL Press; 1992. pp. 75–83.
22. Peirson SN. Quantitative analysis of ocular gene expression. In: Dorak TM (ed.), *Real-time PCR*. New York: Taylor & Francis Group; 2006. pp. 107–126.
23. Peirson SN, Butler JN, Foster RG. Experimental validation of novel and conventional approaches to quantitative real-time PCR data analysis. *Nucleic Acids Res* 2003;**31**:e73–e79.
24. Adams PS. Data analysis and reporting. In: Dorak TM (ed.), *Real-time PCR*. New York: Taylor & Francis Group; 2006. pp. 41–62.
25. Tallquist MD, Soriano P. Cell autonomous requirement for PDGFRalpha in populations of cranial and cardiac neural crest cells. *Development* 2003; **130**:507–518.
26. Chai Y, Jiang X, Ito Y, Bringas P Jr, Han J, Rowitch DH *et al*. Fate of the mammalian cranial neural crest during tooth and mandibular morphogenesis. *Development* 2000;**127**:1671–1679.
27. Saga Y, Kitajima S, Miyagawa-Tomita S. Mesp1 expression is the earliest sign of cardiovascular development. *Trends Cardiovasc Med* 2000;**10**:345–352.
28. Kaufman M, Bard JBL. *The Anatomical Basis of Mouse Development*. San Diego: Academic Press; 1999.
29. Weninger WJ, Mohun T. Phenotyping transgenic embryos: a rapid 3-D screening method based on episcopic fluorescence image capturing. *Nat Genet* 2002;**30**:59–65.
30. Danielian PS, Muccino D, Rowitch DH, Michael SK, McMahon AP. Modification of gene activity in mouse embryos in utero by a tamoxifen-inducible form of Cre recombinase. *Curr Biol* 1998;**8**:1323–1326.
31. Zhang Z, Cerrato F, Xu H, Vitelli F, Morishima M, Vincentz J *et al*. Tbx1 expression in pharyngeal epithelia is necessary for pharyngeal arch artery development. *Development* 2005;**132**:5307–5315.
32. Cai CL, Liang X, Shi Y, Chu PH, Pfaff SL, Chen J *et al*. Isl1 identifies a cardiac progenitor population that proliferates prior to differentiation and contributes a majority of cells to the heart. *Dev Cell* 2003;**5**:877–889.
33. Moorman AF, Christoffels VM. Cardiac chamber formation: development, genes, and evolution. *Physiol Rev* 2003;**83**:1223–1267.
34. Liu C, Liu W, Lu MF, Brown NA, Martin JF. Regulation of left-right asymmetry by thresholds of Pitx2c activity. *Development* 2001;**128**:2039–2048.
35. Gage PJ, Suh H, Camper SA. Dosage requirement of Pitx2 for development of multiple organs. *Development* 1999;**126**:4643–4651.
36. McElhinney DB, Geiger E, Blinder J, Benson DW, Goldmuntz E. NKX2.5 mutations in patients with congenital heart disease. *J Am Coll Cardiol* 2003;**42**:1650–1655.
37. Goldmuntz E, Geiger E, Benson DW. NKX2.5 mutations in patients with tetralogy of fallot. *Circulation* 2001;**104**:2565–2568.
38. Benson DW, Silberbach GM, Kavanaugh-McHugh A, Cottrill C, Zhang Y, Riggs S *et al*. Mutations in the cardiac transcription factor NKX2.5 affect diverse cardiac developmental pathways. *J Clin Invest* 1999;**104**:1567–1573.
39. Bamford RN, Roessler E, Burdine RD, Saplakoglu U, dela Cruz J, Splitt M *et al*. Loss-of-function mutations in the EGF-CFC gene CFC1 are associated with human left-right laterality defects. *Nat Genet* 2000;**26**:365–369.
40. Goldmuntz E, Bamford R, Karkera JD, dela Cruz J, Roessler E, Muenke M. CFC1 mutations in patients with transposition of the great arteries and double-outlet right ventricle. *Am J Hum Genet* 2002;**70**:776–780.
41. Megarbane A, Salem N, Stephan E, Ashoush R, Lenoir D, Delague V *et al*. X-linked transposition of the great arteries and incomplete penetrance among males with a nonsense mutation in ZIC3. *Eur J Hum Genet* 2000; **8**:704–708.
42. Gebbia M, Ferrero GB, Pilia G, Bassi MT, Aylsworth A, Penman-Splitt M *et al*. X-linked situs abnormalities result from mutations in ZIC3. *Nat Genet* 1997;**17**:305–308.
43. Ware SM, Peng J, Zhu L, Fernbach S, Colicos S, Casey B *et al*. Identification and functional analysis of ZIC3 mutations in heterotaxy and related congenital heart defects. *Am J Hum Genet* 2004;**74**:93–105.

44. Shiratori H, Sakuma R, Watanabe M, Hashiguchi H, Mochida K, Sakai Y *et al*. Two-step regulation of left-right asymmetric expression of Pitx2: initiation by nodal signaling and maintenance by Nkx2. *Mol Cell* 2001; **7**:137–149.
45. Yan YT, Gritsman K, Ding J, Burdine RD, Corrales JD, Price SM *et al*. Conserved requirement for EGF-CFC genes in vertebrate left-right axis formation. *Genes Dev* 1999;**13**:2527–2537.
46. Gaio U, Schweickert A, Fischer A, Garratt AN, Muller T, Ozcelik C *et al*. A role of the cryptic gene in the correct establishment of the left-right axis. *Curr Biol* 1999;**9**:1339–1342.
47. Purandare SM, Ware SM, Kwan KM, Gebbia M, Bassi MT, Deng JM *et al*. A complex syndrome of left-right axis, central nervous system and axial skeleton defects in Zic3 mutant mice. *Development* 2002;**129**: 2293–2302.